AFRL-RX-WP-TP-2011-4236

DEVELOPING THE CAPABILITY TO MONITOR SMALL FATIGUE CRACK GROWTH UNDER ELEVATED TEMPERATURE, ULTRA-HIGH VACUUM CONDITIONS (Preprint)

M. J. Caton and A. H. Rosenberger

Metals Branch
Metals, Ceramics & NDE Division

B. T. Gockel

University of Dayton

S. K. Jha and C. J. Szczepanski

Universal Technology Corporation

JULY 2011

AIR FORCE RESEARCH LABORATORY
MATERIALS AND MANUFACTURING DIRECTORATE
WRIGHT-PATTERSON AIR FORCE BASE, OH 45433-7750
AIR FORCE MATERIEL COMMAND
UNITED STATES AIR FORCE

REPORT DOCUMENTATION PAGE

Form Approved
OMB No. 0704-0188

1. REPORT DATE *(DD-MM-YY)*	2. REPORT TYPE	3. DATES COVERED *(From - To)*
July 2011	Journal Article Preprint	01 July 2011 – 01 July 2011

4. TITLE AND SUBTITLE

DEVELOPING THE CAPABILITY TO MONITOR SMALL FATIGUE CRACK GROWTH UNDER ELEVATED TEMPERATURE, ULTRA-HIGH VACUUM CONDITIONS (Preprint)

5a. CONTRACT NUMBER
In-House

5b. GRANT NUMBER

5c. PROGRAM ELEMENT NUMBER
62102F

6. AUTHOR(S)

M. J. Caton and A. H. Rosenberger (Metals Branch, Metals, Ceramics & NDE Division (AFRL/RXLM))
B. T. Gockel (University of Dayton)
S. K. Jha and C. J. Szczepanski (Universal Technology Corporation)

5d. PROJECT NUMBER
4347

5e. TASK NUMBER
20

5f. WORK UNIT NUMBER
LM121100

7. PERFORMING ORGANIZATION NAME(S) AND ADDRESS(ES)

Metals, Ceramics & NDE Division, Metals Branch (AFRL/RXLM)
Materials and Manufacturing Directorate
Air Force Research Laboratory
Wright-Patterson Air Force Base, OH 45433-7750
Air Force Materiel Command, United States Air Force

University of Dayton

Universal Technology Corporation

8. PERFORMING ORGANIZATION REPORT NUMBER
AFRL-RX-WP-TP-2011-4236

9. SPONSORING/MONITORING AGENCY NAME(S) AND ADDRESS(ES)

Air Force Research Laboratory
Materials and Manufacturing Directorate
Wright-Patterson Air Force Base, OH 45433-7750
Air Force Materiel Command
United States Air Force

10. SPONSORING/MONITORING AGENCY ACRONYM(S)
AFRL/RXLM

11. SPONSORING/MONITORING AGENCY REPORT NUMBER(S)
AFRL-RX-WP-TP-2011-4236

12. DISTRIBUTION/AVAILABILITY STATEMENT
Approved for public release; distribution unlimited.

13. SUPPLEMENTARY NOTES
PAO case number 88ABW-2010-5381, cleared 06 October 2010. The U.S. Government is joint author of this work and has the right to use, modify, reproduce, release, perform, display, or disclose the work. Submitted to the Journal of Metals. Document contains color.

14. ABSTRACT

It has been observed that the life limiting fatigue behavior in numerous superalloys is dominated by small crack growth behavior. While environmental effects on crack growth behavior of Ni-base superalloys are well documented within the literature, the published research is largely limited to long crack behavior due to the difficulty of measuring small cracks in a vacuum chamber. A testing capability for optical measurement of small cracks under ultra-high vacuum and at elevated temperatures has been developed. Optical measurement capabilities have been evaluated on a lab air machine to determine crack measurement accuracy. Vacuum tests were then run at 650 °C on Ni-base specimens to quantify the effect of vacuum on the propagation life within the small crack regime. The effectiveness of this test capability and considerations for this technique are discussed.

15. SUBJECT TERMS
Fatigue behavior, crack growth behavior, small cracks, long cracks

16. SECURITY CLASSIFICATION OF:			17. LIMITATION OF ABSTRACT:	18. NUMBER OF PAGES	19a. NAME OF RESPONSIBLE PERSON (Monitor)
a. REPORT	b. ABSTRACT	c. THIS PAGE			Michael J. Caton
Unclassified	Unclassified	Unclassified	SAR	24	19b. TELEPHONE NUMBER *(Include Area Code)* N/A

Standard Form 298 (Rev. 8-98)
Prescribed by ANSI Std. Z39-18

Approved for public release; distribution unlimited.

Developing the Capability to Monitor Small Fatigue Crack Growth Under Elevated Temperature, Ultra-High Vacuum Conditions

B. T. Gockel[a,b], M. J. Caton[a], S. K. Jha[c], C. J. Szczepanski[c], A. H. Rosenberger[a]

[a] *U. S. Air Force Research Laboratory, Wright-Patterson AFB, OH 45433-7817, USA*

[b] *University of Dayton, Dayton, OH 45469, USA*

[c] *Universal Technology Corporation, Dayton, OH 45432, USA*

Abstract

It has been observed that the life limiting fatigue behavior in numerous superalloys is dominated by small crack growth behavior. While environmental effects on crack growth behavior of Ni-base superalloys are well documented within the literature, the published research is largely limited to long crack behavior due to the difficulty of measuring small cracks in a vacuum chamber. A testing capability for optical measurement of small cracks under ultra-high vacuum and at elevated temperatures has been developed. Optical measurement capabilities have been evaluated on a lab air machine to determine crack measurement accuracy. Vacuum tests were then run at 650°C on Ni-base specimens to quantify the effect of vacuum on the propagation life within the small crack regime. The effectiveness of this test capability and considerations for this technique are discussed.

1. Introduction

The design lives of fracture critical components in the aerospace industry are often governed by the minimum behavior. For instance, the US Air Force sets the design life of fracture critical turbine engine components based on the 1 in 1000 probability of the initiation of a crack of a detectable size (typically ~800 μm). Therefore, accurate prediction of minimum lifetimes is needed in order to optimize affordability without jeopardizing safety. Recent studies of turbine engine alloys have shown that the minimum lifetimes are dominated by fatigue crack growth (1), which includes the small crack regime. It has been observed that the influence of loading variables on crack growth behavior can differ significantly between small and long cracks. Figure 1 shows an example of IN100, a Ni-base superalloy, where the effect of dwell loading on the elevated temperature fatigue crack growth behavior is examined. It is seen that a 6 second dwell period has a negligible effect on long crack growth behavior, but results in profoundly faster growth of small cracks. This phenomenon arises from the introduction of time-dependent mechanisms such as creep and environmental attack. However, the degree to which these mechanisms contribute to early crack growth behavior is unknown. One approach to understanding this behavior is to isolate the environment by conducting small fatigue crack growth tests

in vacuum. While a significant amount of research has been conducted to determine the effect of vacuum on long fatigue crack growth, very little has been reported on small fatigue crack growth properties. This paper examines the information currently available in the literature and presents the development of a capability aimed at optically monitoring the early stages of fatigue crack growth behavior (~40μm) up to crack sizes of approximately 2mm under ultra-high vacuum (10^{-9} Torr) at elevated temperatures relevant to turbine engine applications (650^{o}C).

The role of environment on long fatigue crack growth behavior has been examined for decades across numerous materials (2) as illustrated in Table 1. Vasudevan et al. (3) investigated the requirements of a vacuum system to approximate inert conditions. They found that while it varies by material, pressures in the range of 10^{-5} to 10^{-8} Torr often do not represent an inert environment. The importance of minimizing residual gases by use of proper gaskets, efficient pumps and baking the chamber is expressed. While fatigue tests run under vacuum conditions often make use of a chamber surrounding a test frame, another method found in the current literature is building a test frame inside of a scanning electron microscope (SEM) chamber. While these SEM chambers usually only pull vacuum levels of 10^{-6} – 10^{-7} Torr, the ability to monitor significantly smaller cracks with greater resolution is obtained. Both Telesman et al. (4) and Biallas et al. (5) reported environmental effects at these pressures by testing within SEM chambers, but also recognize the limitations of this method, such as specimen geometry, loading frequency and temperature limitations. The ability to take high resolution images of damage mechanisms is the strength of the SEM system, not the ability to isolate environmental effects.

Because each vacuum fatigue test frame is different, multiple types of specimen geometries are reported throughout the current literature, often dictated by material or load frame restrictions. The type of specimen dictates the gripping system needed, as well as size restrictions on the chamber itself. Researchers such as Osinkolu et al. (6) and Kirby et al. (7) utilized single edge notched (SEN) specimens while others such as Reger (8) and Onofrio (9) tested cylindrical and corner crack specimens, respectively. All reported slower crack growth rates in Aluminum and Nickel alloys under vacuum conditions. The majority of the current literature on fatigue crack growth under vacuum utilizes compact tension (C(T)) specimens to monitor long cracks (10-14). This is attributed to the simplification of experimental procedures that these specimens allow. A C(T) specimen is gripped using pin clevises, making load-train alignment simpler. In addition, the crack path is well defined. This allows the crack length to be monitored using a standard technique, such as the direct current potential drop (DCPD) method.

The largest challenge of investigating crack growth rate properties in vacuum is accurately monitoring and measuring the cracks as they grow. Because physical access to the specimen inside the chamber is impossible, remote monitoring systems must be utilized. The DCPD method is, therefore, commonly used on C(T) specimens to monitor long crack growth rates. The limitations of this method are that a prior knowledge of the crack path is required, cracks smaller than 75 μm cannot be resolved, and unintended cracking can occur at the locations where the leads are welded to the specimen (10). Gayda et al. (11) and Holtz et al. (12) both utilized this method on Ni-base alloys and reported environmental effects in the long crack regime. As previously discussed, performing fatigue tests inside

an SEM chamber allows for high resolution imaging of the crack, but comes with size and pressure level restrictions. Another optical method was used by Smith et al. (13) where they took measurements using a traveling, optical microscope. The optical method requires control of where and what direction the crack will grow, such as the case with a C(T) specimen. The crack must initiate and grow in an area that is viewable externally by the microscope.

From the current literature, it was found that few small fatigue crack growth tests run in vacuum have been reported. Biallas et al. (5) investigated the use of environmental SEMs to monitor fatigue crack growth in a variety of materials at temperatures as high as 600^{o}C. They point out that no one specimen size works for all materials and recognize limitations of how high the test frequency can be used with a screw-driven load frame. While they report images of relatively small cracks, the vacuum level inside the test chamber is approximately 10^{-6} Torr, which cannot be considered truly inert. Onofrio et al. (9) report fatigue crack growth data taken at a vacuum level of approximately 10^{-5} Torr. Corner crack specimens were used with a 0.2 mm starter notch and a precrack of 0.1 mm. Because the crack was of known size and location, they were able to use a potential drop method. Petit et al. (14) (15) investigated multiple material systems, looking at both long and small cracks under vacuum levels of approximately 10^{-6} Torr. They report starting crack sizes of approximately 40 µm but it is not clear as to how these cracks were monitored inside the vacuum chamber. It is possible the specimens were removed periodically to replicate the surface or inspect, there exposing them to the environment. The method proposed here utilizes remote monitoring system to prevent any exposure to the environment. The testing system can attain vacuum levels of approximately 10^{-9} Torr with temperatures greater than 1000^{o}C possible at this level. Initial crack sizes will on the order of 40 µm and the crack growth will be monitored until failure.

2. Experimental Development

This section highlights the experimental capabilities necessary to enable small fatigue crack growth tests under ultra-high vacuum. Modifications of both the mechanical and optical monitoring systems were required and as such will be discussed separately.

2.1 Mechanical Testing

Conducting fatigue crack growth tests under elevated temperature and ultra-high vacuum conditions requires three main components: the vacuum chamber and associated pumps, a system for heating the specimen, and a gripping system to grip the specimen. The ultra-high vacuum chamber used in this testing is built around a servohydraulic fatigue testing machine. The chamber itself, seen in Figure 2, is constructed of stainless steel and is double-walled to allow the shell to be heated using a steam generator for burning residual contaminants out of the chamber (3). All flanges, including the front access door, are sealed using ultra-high vacuum grade, hard copper gaskets, and stainless steel bolts. The chamber is evacuated using a two-stage turbomolecular pumping system capable of

maintaining a vacuum of ~1x10^{-9} Torr. Heating of the specimen is done through use of a tungsten mesh furnace with a maximum hot zone temperature of approximately 2200^{o}C (16). Because the system was originally designed to test C(T) specimens, it was necessary to design new grips to allow testing of low cycle fatigue buttonhead specimens inside the chamber. The grips were designed to be identical to standard air-test button-head grips with the exception of the method used for clamping the specimen. A comparison of the old and new style grips can be seen in Figure 3. On a typical load frame, a plunger extends through the inside of the grips to apply pressure to the ends of the specimen between the nut and the plunger. This frame cannot apply hydraulic pressure to the grips due to the integrated design with the vacuum chamber. Thus, a cavity was machined to allow a spacer to be placed at the ends of the specimen, causing the nut to clamp the specimen between the two. While this was not utilized in this study, it allows future testing to be done in the compressive regime without slipping of the specimen. As seen in Figure 4, the specimen sits approximately 12 inches from the shell of the vacuum chamber and is only viewable from the two viewports located on either side of the chamber. It is through these two ports that the optical crack measurements will be taken.

2.2 Optical Monitoring

Because the small fatigue crack specimens are only visible through two viewing ports, the intent was to monitor and measure the crack growth rate utilizing long distance microscopy. This required the cracks to grow in the visible area. Cracks were therefore artificially initiated using Focus Ion Beam (FIB) machined notches. The optical measurements were done using two Questar QM-1 long distance microscopes installed on either side of the chamber. These microscopes are capable of 3 µm resolution when used at the shortest working distance of 22 inches, which allow reliable imaging of crack tip openings. The first step towards utilizing the microscopes to image cracks was to develop a set of optimum lighting conditions. A specimen containing cracks of known sizes was placed on a 3-axis stage and imaged with a QM-1 on a bench to remove as many variables as possible. Different types of lighting, lighting angles and intensity were tested in an attempt to determine optimum settings. These settings were qualitatively inspected through use of the researcher's eye. Because more than one researcher would be using this system, a permanent record of the crack (i.e. a digital picture file) was used to monitor the specimen.

Several camera systems were tested for the purpose of image acquisition and recording including a Nikon D50 single lens reflex (SLR) camera, a research-grade charged coupled device (CCD), and a Microsoft webcam. The SLR camera was found to be unsuitable for the present work because of the vibrations caused by the internal shutter motion during image capture, which significantly reduced the clarity of the image. The CCD camera was also tested but removed from consideration due to the size of the pixels. The next camera to be tested was a Microsoft web camera that was simplified down to the circuit board and CCD. The camera was chosen based on its extraordinarily small pixel size, which is approximately 3 µm. This was placed in a custom built plastic camera body and attached to the microscope system. A number of magnifying lenses were tested for use in the system to optimize the trade-off in magnification and resolution for this application, as seen in Figure 5. A light-through-scope

adapter, which allowed the light source to be focused and shown through the microscopes, and a camera adapter were used throughout the project.

Lighting was a very important aspect in the design of the optical system due to the fact that the vacuum chamber does not contain any light sources. The same access ports used for the microscope must also be used to light the specimen, so it was quickly determined that sending the light through the microscope was the most efficient route. Also, through the same bench-top testing, it was determined that the best images of cracks were achieved by bright, focused light that intersected the specimen face from a perpendicular direction. This focused light simplified the task of aiming and aligning the microscopes while maintaining focus on a 40 µm starter notch at a distance of 22 inches. The light-through-scope adapter gave consistent lighting which allowed consistent images. The lighting source mated to the adapter was a standard, desktop fiber optic light source.

3. Results

3.1 Evaluation of Optical Monitoring System

In order to evaluate the accuracy of the optical system, a room temperature test was performed in laboratory air to determine the accuracy of the measurements and clarity of the images. The specimen was tested at room temperature to avoid the surface oxidation layer induced at elevated temperatures, which has been found to obscure optical measurements of the small cracks. The crack initiation was controlled by use of three 40 µm starter notches placed on one face of a square, buttonhead specimen. All physical constraints presented by the chamber were duplicated on the air test, including placing the viewport glass at the appropriate distance from the microscope. To verify optical measurements, the specimen was replicated using a standard acetate replication method by another researcher. The goal of the test was to evaluate the accuracy of the crack size measurements obtained from the long distance microscope, by comparing these sizes with those obtained from a well established and highly accurate method. However, it was critical that the crack size determination from the images provided by the long distance microscopes not be influenced by knowledge of the true crack sizes. Therefore, the crack size determination from the long distance microscopes and the acetate replication were conducted by separate researchers who did not share these results for the duration of the test. This represents the situation of an actual vacuum test, where there is no physical access to the specimen and the long distance microscopes provide the sole method for crack measurement.

This calibration test was conducted on a super-solvus IN-100 buttonhead specimen. The specimen was tested at a maximum stress of 1150 MPa, a stress ratio of 0.05, and a test frequency of 0.33 Hz. These conditions are representative of those to be run in the vacuum chamber, with the exception of temperature. The specimen had a square gauge section with three FIB-machined micro-notches on one of the flat faces in order to force cracks to start in an area that could be monitored by the microscopes. Figure 6 shows the comparison of the optical measurements and the measurements from replication for the dominant crack.

From the plot, it can be seen that, while not perfect, the two measurement process are in basic agreement. The optical system accurately resolved a 40 µm micro-notch from a distance of 22 inches away and from these notches, small cracks were identified and accurately measured at very small crack lengths, as seen in Figure 6. The two measurement techniques corresponded very well until the crack length reached approximately 200 µm, where it can be seen that it began to diverge. At this crack length, the optical measurement system began to measure cracks in access of the true length by as much as 20–50%. This phenomenon was expected at the smaller crack lengths, not the longer ones. The reason behind this behavior appears to be twofold. The first is that as the surface finishes changes due to plastic deformation from the loading, it introduces artifacts into the optical image that confound the crack tip. While these artifacts do not appear to grow, they can hide the crack if they develop within the crack path. Second, plasticity at the crack tip becomes larger as the crack grows larger. This can obscure the tip of the crack, and due to the subsequent roughness, develop artifacts that cause larger, incorrect crack length measurements to be taken.

Figure 7 shows a comparison of images taken at three different cycle counts and images of the corresponding replicas. The imaging artifacts can be seen in the optical image, yet not in the image of the replica. The image of the replica was taken from an optical microscope. From the long distance microscope image, it can be seen how a crack measurement could be interpreted to be longer than the actual crack length. The crack tip links up with these imaging artifacts and an observer can no longer distinguish between a crack and a deformation-induced feature. It should be noted that when viewed live on a computer screen, the operator has the ability to make fine focus adjustments until accurate decisions can be made about the location of the crack tips. This ability to dial in the image is not something that can represented well in print.

This test suggests that the optical system is a viable way to measure crack lengths in a vacuum chamber when there is no physical access to the specimen. It was particularly encouraging that cracks could be detected at sizes as small as ~45 µm. A potential remedy to the problem of inaccurately measuring the crack length due to misinterpreting imaging artifacts is to characterize the entire area where the crack will propagate to prior to testing. This allows the observer to compare the images and better differentiate between crack length and “features” appearing on the surface. Also, the final crack size can be determined through post-mortem analysis of the fracture surface. This measurement can be used to ensure the final crack measurement made by the optical system is indeed correct. Another method of increasing the accuracy of the optical measurements explored was fracture surface marking. While this has been reported previously in the literature (17), it was unknown the degree to which the fracture surface would mark in the absence of environmental interaction. Initial success was achieved by changing the temperature, stress ratio, and frequency of the test, but this method could not be replicated and therefore requires further investigation.

3.2 Demonstration of Integrated Vacuum Testing Capability

Two vacuum crack growth tests were run in order to demonstrate the integration of the new gripping system, the vacuum test machine, and the optical measurement system. The buttonhead specimens tested were sub-solvus IN100 and machined with a square gage section with nominal cross-sectional dimensions of 4.6mm by 4.6mm. Two micro-notches were FIB machined on opposing sides such that they could be monitored using the long distance microscope system. The test conditions were the same as the previous air test except the test temperature was increased to 650°C (i.e., σ_{max}=1150 MPa, R=0.05, 0.333Hz). The vacuum level on both tests was approximately 10^{-9} Torr. Both tests demonstrated longer fatigue lifetimes when compared to data acquired previously in air, which can be seen in Figure 8. Neither specimen failed from the focused ion beam machined micro-notch. The first test failed from a non-metallic particle (NMP) contained on the surface, which can be seen on the fracture surface shown in Figure 9. The second vacuum test was declared a runout and suspended when no failure was observed after 10^6 cycles. The notches were monitored throughout both tests, and the operator was fully aware of the lack of crack initiation and growth at the notches. This helped confirm that the optical microscopes could accurately monitor the notches.

While the fatal cracks did not grow from the notches, both specimens demonstrated longer fatigue lifetimes then those specimens that have been tested under identical conditions in a laboratory air environment. The specimen that failed from the NMP had a lifetime that was approximately 5.5x longer than what would be conventionally predicted by a conservative life prediction code. Also, the lowest life shown in Figure 8 failed from a crack that initiated from the NMP shown in Figure 10. This NMP is much smaller yet had a shorter total life. The specimen that was declared a runout showed approximately an order of magnitude increase in life compared to other similar tests. This effect appears to be due to the lack of environmental interaction, displaying the importance of developing the capability to quantify the effect on small crack growth.

4. Considerations

4.1 Cleanliness

In running low cycle fatigue crack growth tests under ultra-high vacuum conditions at elevated temperature, there are many considerations that must be taken into account. If an ultra-high vacuum is being pulled on a system, the cleanliness of the system will play a role in the final vacuum level. Any oils or dirt inside the system can hold air particles that negatively affect the level of the vacuum. To combat this, gloves must be worn at all times while working inside the chamber and all tools and fixturing should be cleaned using ethyl alcohol or a similar cleaning solution. Also, during the initial pump-down, the outer shell of the system should be heated to assist in breaking free or burning off any residual dirt or oil. The preparation of the system can dictate whether the vacuum level is high or ultra-high.

4.2 Alignment and Surface Finish

Because the fixturing of the load train must be contained within a chamber, the load train is inherently longer than on a standard MTS machine. This can cause the act of aligning the system to be

much more labor intensive than on a standard machine as well as have more variability than usual. While it was found to be a non-issue with the current testing, more sensitive specimen geometries or materials may find the lack of repeatability to be a problem. This also leads to issues with aligning the specimen's desired viewable area with available viewing ports. Care must be taken to ensure that flat sides must be kept square to the viewports. Also, it was found on the test run at room temperature that due to the yielding of the material on the first load cycle, surface deformation occurred on a significant level. While this deformation was measured to be less than 10 μm, it severely reduced the clarity of the images. This is true for the initial surface preparation for the specimen as well. It is recommended to polish the surface to as smooth and uniform a finish as possible. The severity of these issues would change based on the material being tested, so to some this could be either a non-issue or to others a dead end.

4.3 Vibration

Finally, an issue inherent in many vacuum systems is vibration caused by the turbo or roughing pumps. Because the measurement process is using optical microscopes with image capturing devices attached, vibration can have a negative impact on the image quality. This causes inaccurate measurements to be taken and can skew final results. To combat this, the microscopes need to be isolated from the system using both vibration dampening material as well as stands that have a large mass. A significantly heavy stand, if combined with dampening material, can successfully combat vibration caused by the pumps and enable satisfactory images to be obtained.

5. Conclusions

The development and implementation of an integrated mechanical and optical system to enable the measurement of small fatigue crack growth ($2c \geq 40\mu m$) under ultra-high vacuum (~10^{-9} Torr) has been presented and discussed. The following conclusions can be drawn:

- A mechanical system capable of gripping a buttonhead specimen inside an ultra-high vacuum chamber (~10^{-9} Torr) was developed such that fatigue crack growth tests could be run at elevated temperature in both tension and compression.
- A long distance microscopy system was developed to accurately monitor small fatigue crack growth from a distance of 22" from the specimen surface. Crack initiation was controlled using FIB machined notches of approximately 40 μm.
- Initial evaluation of the long distance microscopy system on a fatigue crack growth test run in laboratory air demonstrated that the optical method could successfully resolve crack sizes down to 40 μm.
- Initial fatigue results showed enhanced fatigue resistance under vacuum conditions in a Ni-base superalloy at elevated temperature for natural initiation from a non-metallic particle. Under conditions examined, crack growth from 40 μm micro-notches was not observed.

- It was shown that one must take care to address multiple factors when attempting to take optical measurements of small cracks from a distance. It was found that specimen surface finish, vibration, and lighting are all key elements to consider and optimize for optimum results.

References

1. *Mean vs. Life-Limiting Fatigue Behavior of a Nickel-Base Superalloy.* **Jha, S. K., Caton, M. J. and Larsen, J. M.** s.l. : Superalloys 2008. pp. 565 - 572.

2. *The Effect of Vacuum on Fatigue Crack Growth.* **Grinberg, N. M.** s.l. : International Journal of Fatigue, 1982.

3. *Analysis of Vacuum Fatigue Crack Growth Results and Its Implications.* **Vasudevan, A. K., Sadananda, K. and Holtz, R. L.** s.l. : International Journal of Fatigue, 2005, Vol. 27.

4. *Fatigue crack growth behavior of a single crystal alloy as observed through an in situ fatigue loading stage.* **Telesman, J. and Kantzos, P.** Dayton : SAMPE, 1988.

5. *In-situ fatigue in an environmental scanning electron microscope - Potential and current limitations.* **Biallas, G. and Maier, H. J.** 2007, International Journal of Fatigue, pp. 1413-1425.

6. *Fatigue Crack Growth in Polycrystalline IN 718 Superalloy.* **Osinkolu, G. A., Onofrio, G. and Marchionni, M.** s.l. : Materials Science & Engineering A, 2003, Vol. 356.

7. *Slow fatigue crack growth and threshold behaviour in air and vacuum of commercial aluminium alloys.* **Kirby, B. R. and Beevers, C. J.** s.l. : Fatigue of Engineering Materials, 1979, Vol. 1.

8. *High Temperature, Low Cycle Fatigue of IN-100 Superalloy II: Influence of Frequency and Environment at High Temperatures.* **Reger, M. and Remy, L.** s.l. : Materials Science & Engineering A, 1988, Vol. 101.

9. *Fatigue Crack Growth of UDIMET 720 Li Superalloy at Elevated Temperature.* **Onofrio, G., Osinkolu, G. A. and Marchionni, M.** s.l. : International Journal of Fatigue, 2001, Vol. 23.

10. *Direct Current Electrical Potential Measurement of the Growth of Small Cracks.* **Gangloff, R. P., et al.** [ed.] J. M. Larsen and J. E. Allison. s.l. : ASTM STP1149-EB, 1992.

11. **Gayda, J., Gabb, T. P. and Miner, R. V.** *Fatigue crack growth propagation of Nickel-Base Superalloys at 650 C.* s.l. : NASA, 1985.

12. *Fatigue threshold maps of PWA 1480 superalloy single crystal in air and vacuum at room temperature.* **Holtz, R. L. and Sadananda, K.** s.l. : TMS, 1997, Vol. High Cycle Fatigue of Structural Materials.

13. *Effect of Environment on Fatigue Crack Propagation Behavior of Alloy 718 at Elevated Temperatures.* **Smith, H. H. and Michel, D. J.** s.l. : Metallurgical Transactions A, 1985, Vol. 17.

14. *Influence of Environment on Small Fatigue Crack Growth.* **Petit, J.** 1999.

15. *Influence of Environment on the Propagation of Short Fatigue Cracks in a Titanium Alloy.* **Petit, J., et al.** s.l. : Short Fatigue Cracks, 1992.

16. *Effects of Microstructure, Temperature and Environmental on Fatigue Crack Growth in Ti-46.5AL-3Nb-2Cr-0.2W Titanium Aluminide.* **Rosenberger, A. H., Worth, B. D. and Larsen, J. M.** s.l. : The Minderals, Metals & Materials Society, 1997. Structural Intermetallics 1997.

17. *Cycle counting for fatigue crack growth analysis.* **Sunder, R., Seetharam, A. and Bhaskaran, T. A.** s.l. : International Journal of Fatigue, 1984, Vol. 6.

18. *Small Fatigue Crack Growth and Failure Mode Transitions in a Ni-Base Superalloy at Elevated Temperature.* **Caton, M. J. and Jha, S. K.** s.l. : Accepted for publication, International Journal of Fatigue.

19. *Frequency Effects on Fatigue Crack Growth Behavior in a Near Alpha Titanium Alloy.* **Ghonem, H. and Foerch, R.** s.l. : Materials Science and Engineering, 1991.

20. *Elevated Temperature Fatigue Crack Growth in Alloy 718--Part II: Effects of Environmental and Material Variables.* **Ghonem, H., Nicholas, T. and Pineau, A.** s.l. : Fatigue & Fracture of Engineering Materials & Structures, 1993, Vol. 16.

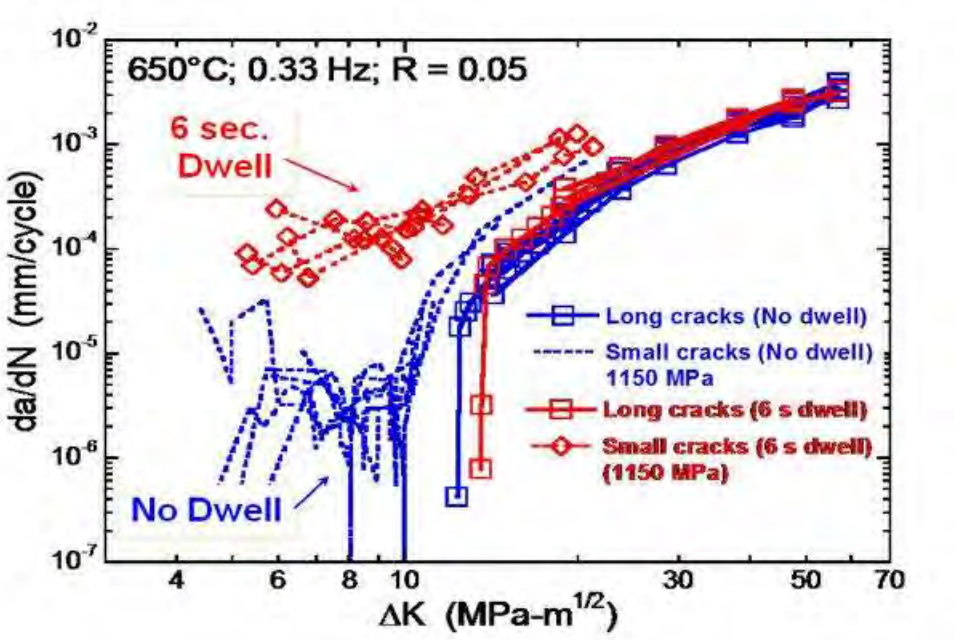

Figure 1. Comparison of dwell and no dwell crack growth rates for IN100 (18)

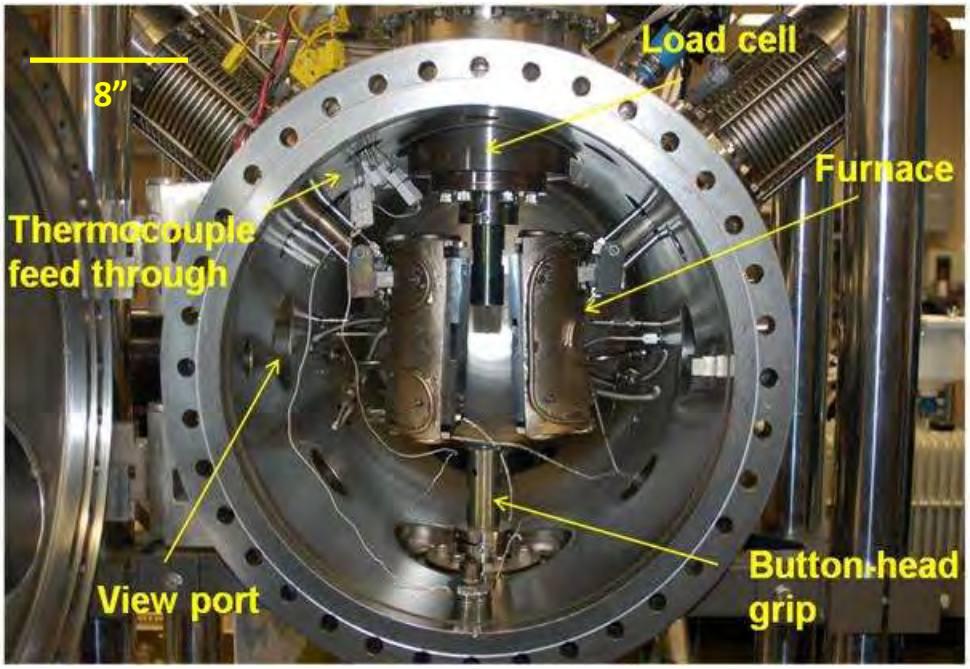

Figure 2. Internal view of ultra-high vacuum system

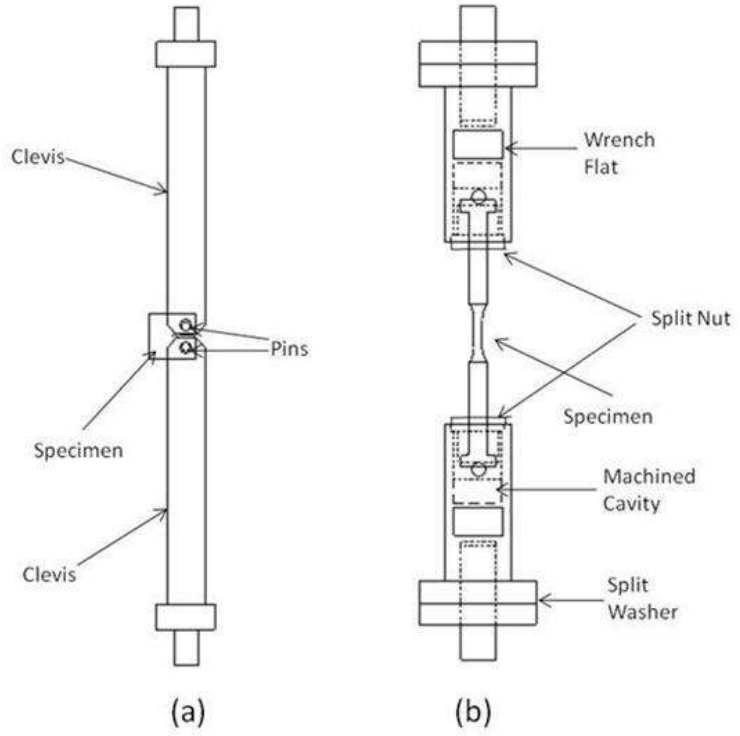

Figure 3. (a) C(T) gripping system, (b) button-head gripping system

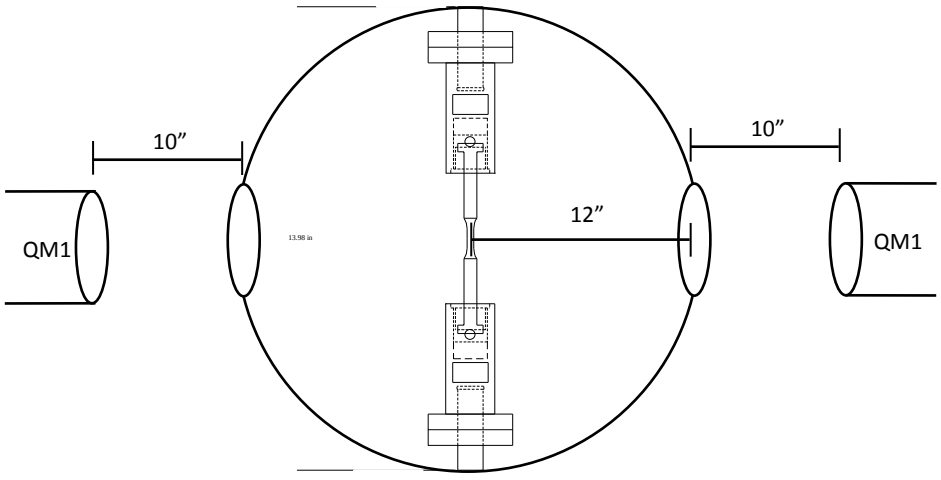

Figure 4. Schematic of optical viewing system outside of vacuum system

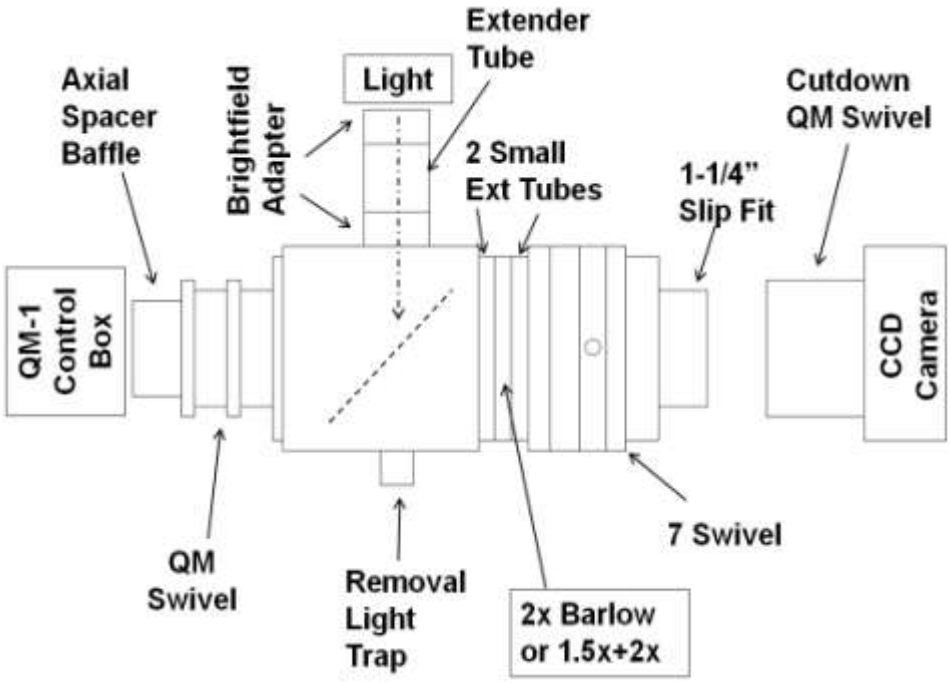

Figure 5. Diagram of optical system

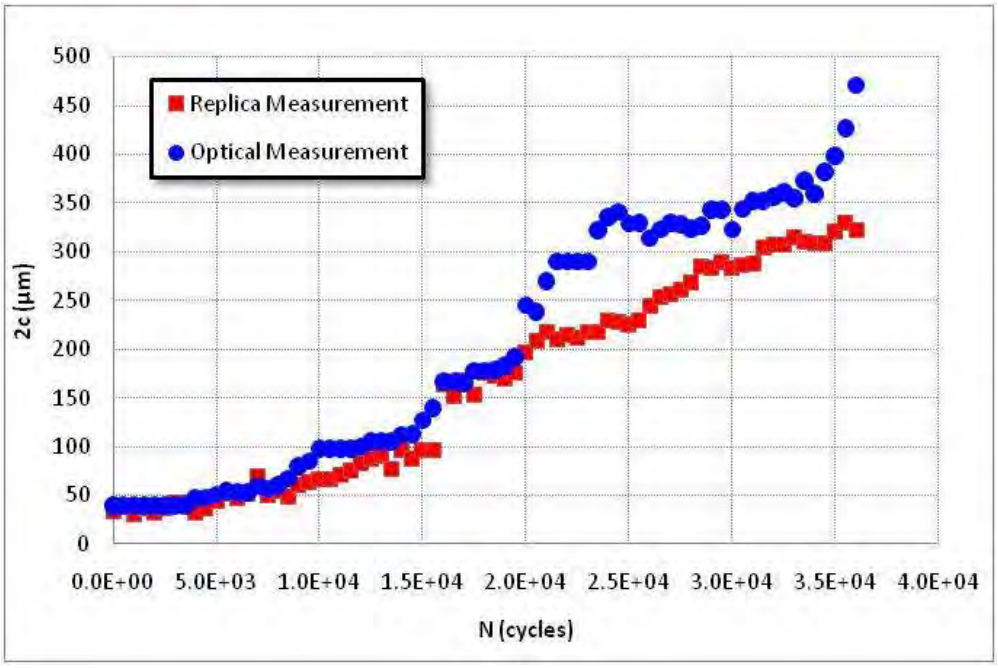

Figure 6. Comparison of Optical and replica measurements

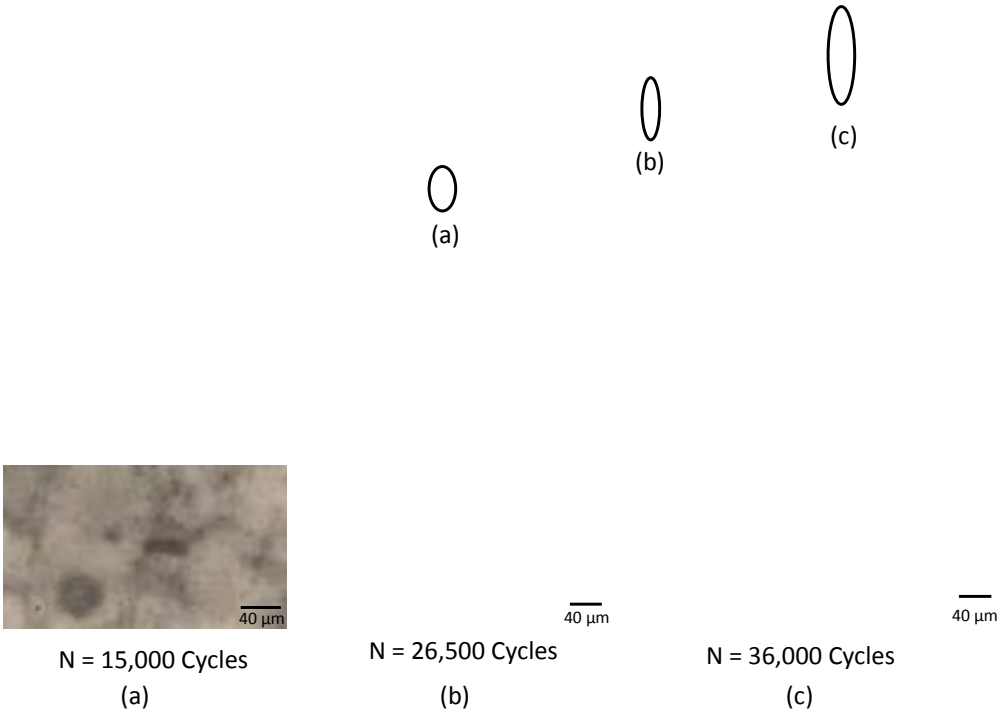

Figure 7. Comparison of replica and optical images at (a) 15,000 cycles (b) 26,500 cycles (c) 36,000 cycles

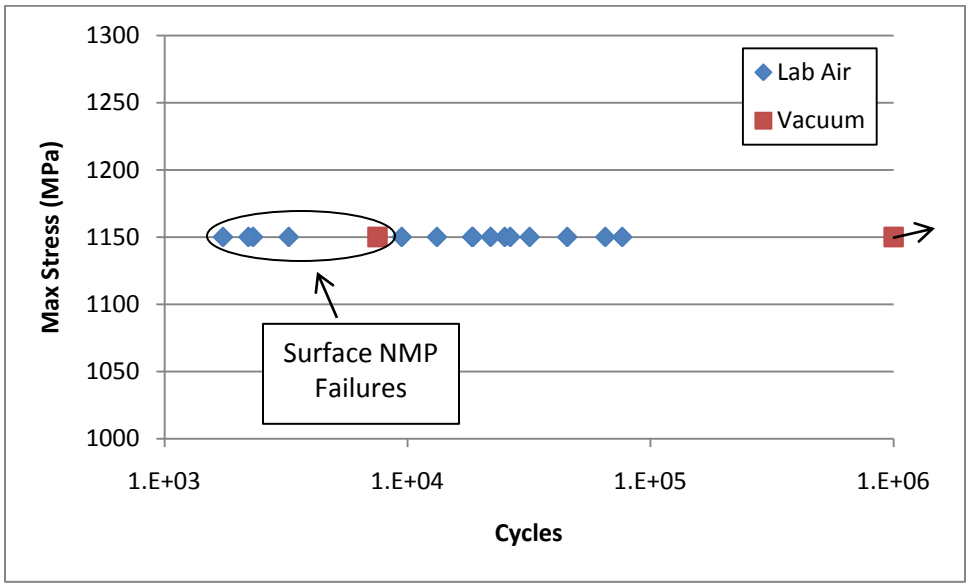

Figure 8. S-N data from air and vacuum small fatigue crack growth tests (1)

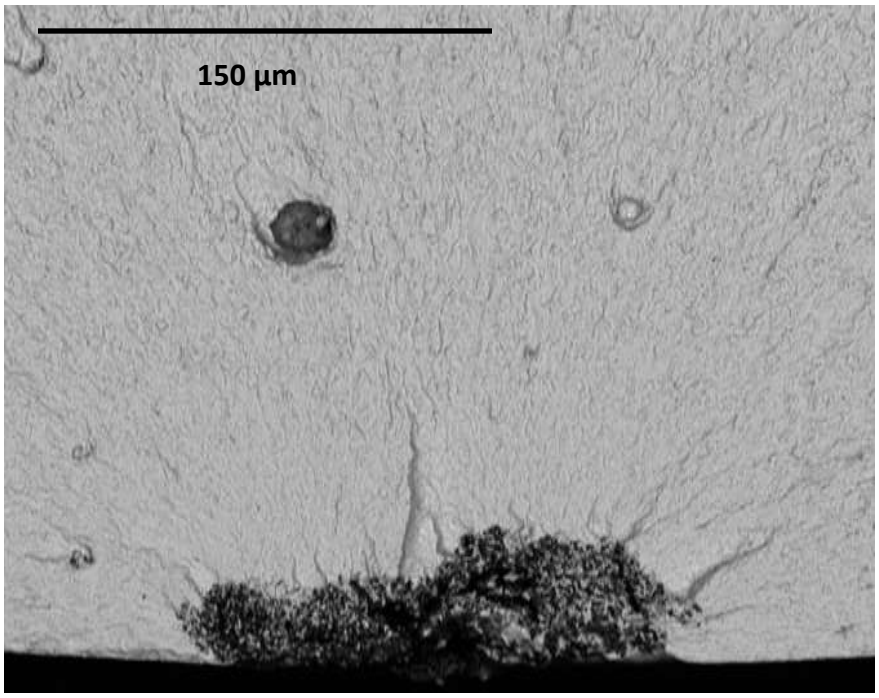

Figure 9. Surface non-metallic particle from vacuum test

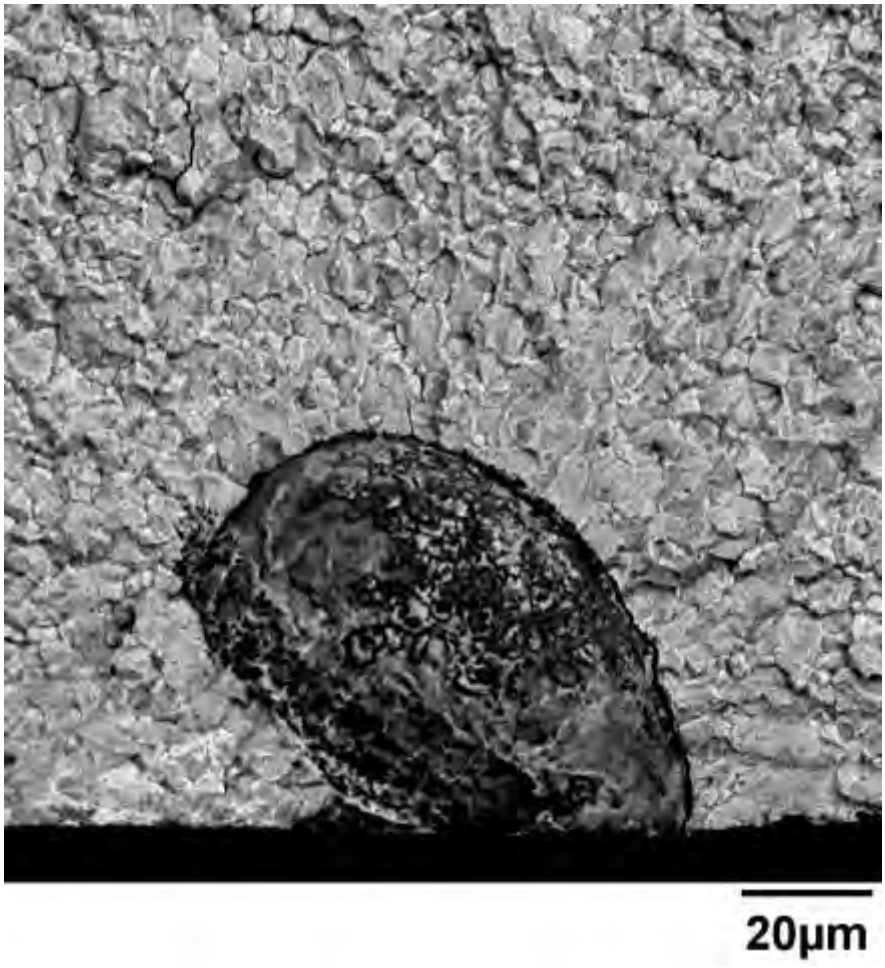

Figure 10. Surface non-metallic particle from laboratory air test

Table 1. Review of vacuum crack growth literature

Author	Material	Vacuum Level (Torr)	Maximum Temperature (°C)	Crack Size (μm)	Specimen Geometry	Measurement Process
Rosenberger et al. (16)	TiAl-base Alloy	2.25E-09	800	> 1 mm	C(T)	CMOD
Osinkolu et al. (6)	In 718	7.50E-05	650	> 1 mm	SENT	DCPD
Biallas et al. (5)	AM60B, Ti alloy	7.40E-06	750	Not Specified	Flat Dogbone	SEM
Smith et al. (13)	In 718	5.00E-08	650	> 1 mm	C(T)	Optically
Onofrio et al. (9)	UDIMET 720 Li	7.50E-05	700	> 300 μm	Corner Crack	DCPD
Reger et al. (8)	IN100	1.50E-05	1000	> 600 μm	Cylindrical	A.C. Potential Drop
Kirby et al. (7)	Al Alloys	1.00E-06	Room	> 1 mm	SENT	DCPD
Holtz et al. (12)	Ni Alloy	4.00E-07	Room	> 1 mm	C(T)	DCPD
Ghonem et al. (19)	Ti Alloy	5.00E-08	550	> 1 mm	C(T)	DCPD
Ghonem et al. (20)	In 718	1.00E-08	650	> 1 mm	C(T)	Not Specified
Gayda et al. (11)	Ni Alloys	1E-5 - 1E-6	650	> 1 mm	C(T)	DCPD
Telesman et al. (4)	Ni Alloy	1.50E-07	Room	> 800 μm	SENT	SEM
Petit et al. (14) (15)	Al, Ti, Steel Alloys	3.75E-06	Room	> 40 μm	C(T), Custom	Replication